

Active, Versatile, and Removable Iron Catalysts with Phosphazanium Salts for Living Radical Polymerization of Methacrylates¹

Muneki Ishio,[†] Masao Katsube,[†] Makoto Ouchi,[†] Mitsuo Sawamoto,^{*,†} and Yoshihisa Inoue[‡]

Department of Polymer Chemistry, Graduate School of Engineering, Kyoto University, Katsura, Nishikyo-ku, Kyoto 615-8510, Japan, and Research Center, Mitsui Chemical, Inc., 580-32 Nagaura, Sodegaura, Chiba 299-0265, Japan

Received August 3, 2008; Revised Manuscript Received November 4, 2008

ABSTRACT: Phosphazanium halides (PZN–X; X = Cl, Br, I), highly delocalized bulky salts, turned out to be excellent cocatalysts to be combined with iron halides (FeX₂) to form in situ active anionic Fe(II) complexes that effectively catalyze living radical polymerization of alkyl and functionalized methacrylates with improved catalytic activity and tolerance to polar functionalities. For example, equimolar combinations of FeBr₂/PZN–Br efficiently induced a living radical polymerization of methyl methacrylate (MMA) with a bromide initiator [H–(MMA)₂–Br] to give polymers with controlled molecular weights and narrow molecular weight distributions ($M_w/M_n < 1.2$). Polymer molecular weight could be extended upon addition of second feeds of monomer or at lower initiator dose, while retaining narrow distributions. In terms of activity and controllability, the PZN-based catalysts were thus predominantly distinguished from not only a conventional iron complex [FeBr₂(PPh₃)₂; Ph = C₆H₅] but also other hitherto known combinations of FeBr₂ with such an onium salt as tetrabutylammonium or phosphonium bromide, as further demonstrated by their reversible and hysteresis-free redox cycles with lower oxidation and reduction potentials (cyclic voltammetry). The new iron catalysts could be readily removed from as-prepared polymer solutions by simple washing with water to give virtually colorless products with the metal residue below 5 ppm.

Introduction

Design criteria for transition metal complex catalysts in organic and polymerization reactions often involve conflicting factors of primary importance starting with feasibility, activity, selectivity, substrate versatility, and functionality tolerance, along with those particularly important upon actual applications, removability, recyclability, durability, and cost. Additional considerations currently prevailing include environmental friendliness, safety (toxicity), and global abundance (availability). From these multifaceted viewpoints, iron (Fe) would be a promising central metal for catalysts, potentially active, highly abundant, readily recoverable, and relatively nontoxic.²

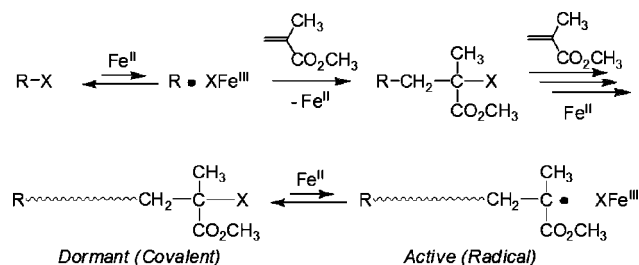
“Transition metal-catalyzed living radical polymerization”³ is one of such catalyzed reactions where metal catalysts critically contribute to the precision control of radical polymerization to give polymers of well-defined molecular weight, architecture, and functionality (Scheme 1).^{3,4} Therein a metal catalyst activates an initiator (R–X) bearing a carbon–halogen bond for homolysis cleavage, where the metal center itself is one-electron oxidized. The primary radical species (R•) thus generated initiates radical propagation with some monomers to grow into a polymer chain, and afterward the oxidized catalyst returns the halogen to the growing radical to regenerate a terminal carbon–halogen (dormant species), while it is one-electron reduced to return to the original lower-valence state complex. To achieve living polymerization, the activation–deactivation process should be reversible and far favored to the dormant species so as to retain an extremely low radical concentration and to suppress bimolecular radical termination, relative to radical propagation. Obviously, the efficiency depends on the metal catalyst, which is modified by the combination of a central metal and ligands, in accordance with the structure of dormant species derived from monomer and leaving halogen. So far, a

large variety of catalysts have been developed worldwide, where the central metals are primarily confined to ruthenium³ and copper,⁵ with nickel,⁶ iron,^{7–19} and other late transition metals acquiring renewed attention.

Iron complexes, undergoing oxidation/reduction cycle by one electron, have already been demonstrated to catalyze living radical polymerization, since the first example with a divalent iron chloride coordinated by triphenylphosphine [FeCl₂(PPh₃)₂].⁷ As with other metal complexes, their catalytic performance such as activity and controllability clearly depends on ligands, which now also include bipyridine,⁸ cyclopentadiene,⁹ pentamethylcyclopentadiene,¹⁰ isophthalic acid,¹¹ imidazolidene,¹² diimine,¹³ diiminopyridine,¹⁴ salicylaldiminato,¹⁵ pyridylphosphine,¹⁶ triazacyclononane,¹⁷ alkyl phosphine,¹⁸ and bis(oxazoline),¹⁹ among many others. In addition to their inherent advantages of abundance and benignity, some iron catalysts are readily removed from the products by simply washing with water.

However, as polymerization catalysts, iron complexes seem generally inferior to the ruthenium or copper counterparts. For example, some iron complexes show lower activity for polymerization of methacrylates, even though they effectively work for acrylates and styrenes. It is more serious that most of them are unable to catalyze living polymerizations of functional monomers directly because they readily interact with polar

Scheme 1



* Corresponding author. E-mail: sawamoto@star.polym.kyoto-u.ac.jp.

[†] Kyoto University.

[‡] Mitsui Chemical, Inc.

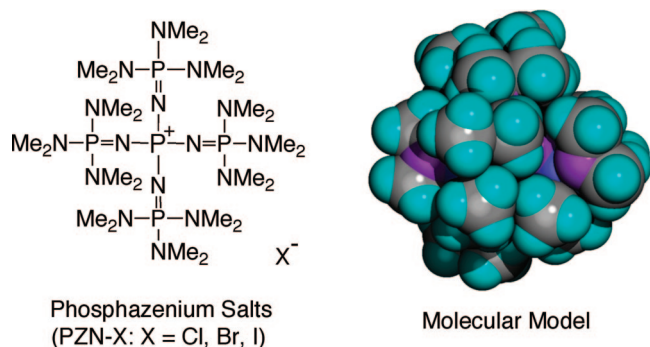


Figure 1. Structures of phosphazanium salts. Colors in atom labeling: green (hydrogen), gray (carbon), purple (nitrogen), and blue (phosphorus).

groups to lose their catalytic activity. Actually, few iron catalysts have been reported active for polar monomers.

Herein we therefore directed attention to “anionic” iron complexes as catalysts from the viewpoint that the higher electron density of the metal center would possibly enhance catalytic activity as well as tolerance to electron-rich polar functional monomers. For this we have employed phosphazanium salts²⁰ (PZN-X; X = Cl, Br, I; Figure 1) as anion resources for iron(II) halides (FeX_2) to achieve living radical polymerization of methyl methacrylate (MMA) or functional monomers with higher controllability and activity. PZN-X salts were originally designed as nonmetallic molecular catalysts for nucleophilic substitution reactions or ring-opening reactions of oxiranes with aryl carboxylates, and structurally they are characterized by the bulky, dendritic, conjugated cation (ca. 12 Å in diameter) where the positive charge is highly delocalized, effectively rendering it non-nucleophilic and well separated from the halide anion, both spatially and electronically.

Similar salt-based Fe(II) catalysts have in fact been reported for living radical polymerization,²¹ in which tetraalkylammonium and -phosphonium salts are combined with FeBr_2 , but their overall activity appears not so high (incomplete monomer conversion), most likely because of the heterogeneity in polymerization media.

In this work, we examined the suitable conditions of iron halide/phosphazene ($\text{FeX}_2/\text{PZN-X}$) catalyst systems for living radical polymerization of MMA. Equimolar combinations of bromide derivatives, in conjunction with a bromide initiator [e.g., $\text{H-(MMA)}_2\text{-Br}$], induced living polymerization where the catalytic activity is clearly superior to conventional neutral phosphine complexes [e.g., $\text{FeBr}_2(\text{PPh}_3)_2$] or the anionic ammonium and phosphonium FeBr_2 salts.

Experimental Section

Materials. MMA (TCI; purity >99%) was dried overnight over calcium chloride and purified by double distillation from calcium hydride before use. The MMA dimeric initiators [$\text{H-(MMA)}_2\text{-X}$; X = Cl,²² Br²³] were prepared according to literature. Iron bromide (Aldrich; purity >98%), iron chloride (Kanto Kagaku >97%), tetrabutylammonium bromide (TCI, >98%), tetrabutylphosphonium bromide (TCI >99%), and tetraphenylphosphonium bromide (TCI >98%), were used as received and handled in a glovebox (M. Braun Labmaster 130) under a moisture- and oxygen-free argon atmosphere (H_2O <1 ppm; O_2 <1 ppm). The phosphazanium salts were received from Mitsui Chemical, Inc.²⁴ and handled in a glovebox. THF was passed through purification columns (solvent dispensing system) and bubbled with dry nitrogen for more than 15 min immediately before use. *n*-Octane (internal standard for gas chromatography) was dried over calcium chloride and distilled calcium hydride.

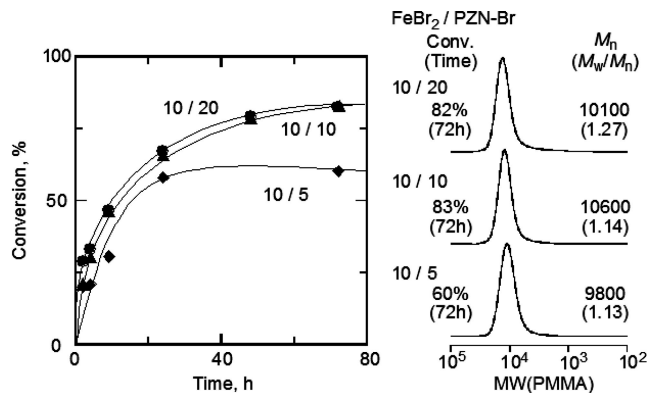


Figure 2. Effects of phosphazene/iron ratio on living radical polymerization of MMA with $\text{H-(MMA)}_2\text{-Br}/\text{FeBr}_2/\text{PZN-Br}$ in THF at 60 °C: $[\text{MMA}]_0 = 2000 \text{ mM}$; $[\text{H-(MMA)}_2\text{-Br}]_0 = 20 \text{ mM}$; $[\text{FeBr}_2]_0 = 10 \text{ mM}$; $[\text{PZN-Br}]_0 = 5.0$ (◆), 10 (▲), and 20 mM (●).

Polymerization Procedures. Polymerization was carried out by the syringe technique under dry argon in baked glass tubes equipped with a three-way stopcock or in sealed glass vials. A typical procedure for MMA polymerization with $\text{H-(MMA)}_2\text{-Br}/\text{FeBr}_2/\text{PZN-Br}$ was as follows. In a 50 mL round-bottom flask, FeBr_2 (9.7 mg, 0.045 mmol), PZN-Br (36.9 mg, 0.045 mmol), and THF (3.23 mL) were added under dry argon and stirred at 60 °C in 5 min. After cooling to room temperature, *n*-octane (0.12 mL), MMA (0.96 mL, 9 mmol), and $\text{H-(MMA)}_2\text{-Br}$ (0.19 mL of 480 mM in toluene, 0.09 mmol) were added sequentially under dry argon. The total volume of reaction mixture was thus 4.5 mL. Immediately after mixing, aliquots (0.60 mL each) of the solution were injected into glass tubes which were then sealed (except when a stopcock was used) and placed in an oil bath kept at desired temperature. In predetermined intervals, the polymerization was terminated by cooling the reaction mixtures to −78 °C. Monomer conversion was determined from the concentration of residual monomer measured by gas chromatography with *n*-octane as an internal standard. The quenched reaction solutions were diluted with toluene (ca. 20 mL), washed with water three times, and evaporated to dryness to give the products that were subsequently dried overnight under vacuum at room temperature.

Measurement. The molecular weight distribution, M_n , and M_w/M_n values of polymers measured in chloroform at 40 °C on three polystyrene gel columns [Shodex K-805 L (pore size: 20–1000 Å; 8.0 mm i.d. × 30 cm) × 3; flow rate 1.0 mL/min] connected to a Jasco PU-980 precision pump and a Jasco 930-RI refractive index detector and 970-UV ultraviolet detector. The columns were calibrated against 13 standard PMMA samples (Polymer Laboratories; $M_n = 630\text{--}1\,200\,000$, $M_w/M_n = 1.06\text{--}1.22$) as well as the monomer. ^1H NMR spectra of the obtained polymers were recorded in CDCl_3 at 25 °C on a JEOL JNM-LA500 spectrometer operating at 500.16 MHz. Polymers for ^1H NMR analysis were fractionated by preparative SEC (column: Shodex K-2002).

Cyclic voltammograms were recorded by using a Hokuto Denko HZ-3000 apparatus. The sample preparation for $\text{FeBr}_2/\text{PZN-Br}$ catalyst is described. FeBr_2 (8.6 mg, 0.040 mmol), PZN-Br (32.8 mg, 0.040 mmol), and THF (8 mL) were added sequentially in a baked glass tube equipped with a three-way stopcock under argon and stirred at 60 °C for 3 h. After heating, solvent was evaporated, and a solution of *n*-Bu₄NPF₆ (supporting electrolyte) in $\text{CH}_2\text{ClCH}_2\text{Cl}$ solution (100 mM, 8 mL) was added into the tube under argon. Measurements were carried out at 0.1 V s^{−1} under argon. A three-electrode cell was used which was equipped with a platinum disk as a working electrode, a platinum wire as a counter electrode, and an Ag/AgCl electrode as a reference.

Results and Discussion

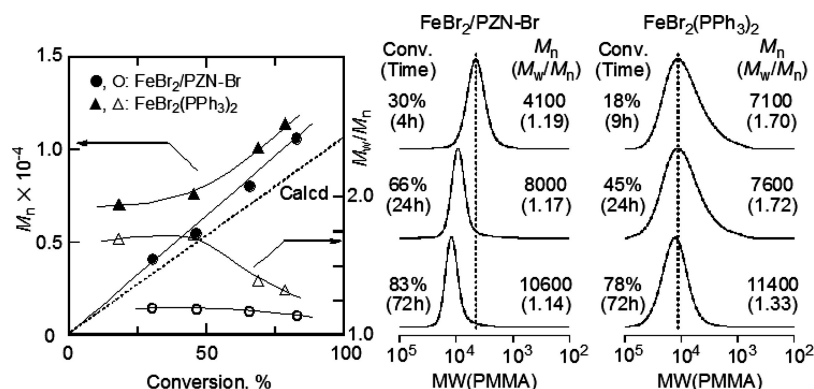
Effects of Polymerization Conditions: FeBr_2 /Phosphazene Ratio and Polymerization Temperature. First, we examined effects of FeBr_2 /phosphazanium bromide (PZN-Br) ratio on

Table 1. Effects of Temperature on Living Radical Polymerization of MMA with H-(MMA)₂-Br/FeBr₂/PZN-Br^a

entry	initiator	iron halide	phosphazene	temp (°C)	time (h)	conv (%)	<i>M_n</i>	<i>M_w/M_n</i>
1	H-(MMA) ₂ -Br	FeBr ₂	PZN-Br	80	72	73	6 700	1.55
2	H-(MMA) ₂ -Br	FeBr ₂	PZN-Br	60	72	83	10 600	1.14
3	H-(MMA) ₂ -Br	FeBr ₂	PZN-Br	40	72	81	7 600	1.17

^a [MMA]₀ = 2000 mM, [initiator]₀ = 20 mM, [iron halide]₀ = 10 mM, [phosphazene]₀ = 10 mM in THF.**Table 2. Comparisons of Initiator, Iron halide, and Phosphazene on Living Radical Polymerization of MMA^a**

entry	initiator	iron halide	phosphazene	temp (°C)	time (h)	conv (%)	<i>M_n</i>	<i>M_w/M_n</i>
1	H-(MMA) ₂ -Br	FeBr ₂	PZN-I	60	72	84	14 200	1.20
2	H-(MMA) ₂ -Br	FeBr ₂	PZN-Br	60	72	83	10 600	1.14
3	H-(MMA) ₂ -Br	FeBr ₂	PZN-Cl	60	72	74	9 300	1.38
4	H-(MMA) ₂ -Cl	FeBr ₂	PZN-Br	60	72	92	12 000	1.92
5	H-(MMA) ₂ -Br	FeCl ₂	PZN-Br	60	72	77	12 400	1.53
6	H-(MMA) ₂ -Cl	FeCl ₂	PZN-Cl	60	72	83	14 200	1.73

^a [MMA]₀ = 2000 mM, [initiator]₀ = 20 mM, [iron halide]₀ = 10 mM, [phosphazene]₀ = 10 mM in THF.**Figure 3.** Comparison of FeBr₂/PZN-Br with FeBr₂(PPh₃)₂ on living radical polymerization of MMA in THF at 60 °C: [MMA]₀ = 2000 mM; [H-(MMA)₂-Br]₀ = 20 mM; [iron catalyst]₀ = 10 mM. Iron catalyst: FeBr₂/PZN-Br (●, ○); FeBr₂(PPh₃)₂ (▲, △).

the polymerization of MMA coupled with bromide initiator [H-(MMA)₂-Br] in THF at 60 °C, where the [FeBr₂]₀/[PZN-Br]₀ was changed to be 10/5, 10/10, and 10/20 mM for [MMA]₀/[H-(MMA)₂-Br]₀ = 2000/20 mM (Figure 2). Polymerization proceeded in homogeneous system under every condition, and the rate was dependent on the ratio: the less feed of phosphazene than FeBr₂ ([FeBr₂]₀/[PZN-Br]₀ = 10/5 mM) resulted in relatively slow polymerization and retardation at the latter stage, while the equimolar and twice feed induced smooth polymerization without such deactivation. Interestingly, the molecular weights were fairly controlled regardless of the conditions, although the molecular weight distributions became slightly broader with more feed of phosphazene ($M_w/M_n > 1.25$). These results would suggest that the equimolar ratio is suitable for control in this system and possibly FeBr₂ forms an ionic complex, [FeBr₂X]⁻,²⁵ with equimolar phosphazene to catalyze the controlled polymerization.

Then, we also investigated effects of polymerization temperature (Table 1). Increasing temperature from 60 to 80 °C resulted in worse control, giving broader molecular weight distributions [M_w/M_n = 1.14 (60 °C) vs 1.55 (80 °C)], which would be caused by the low thermal stability of the catalyst or the oxidized form. Interestingly, even at 40 °C, the polymerization proceeded to give controlled PMMA, suggesting the catalyst generated from FeBr₂/PZN-Br is potentially active.

Effects of Halogen: Initiator, Iron Halide, and Phosphazene Salt. In transition-metal-catalyzed living radical polymerization, the halogen in growing terminal is likely exchanged with that of catalyst during the repeating activation process, as already confirmed by ¹H NMR analyses.^{22,23} Different halogen combination in initiator/catalyst gives rise to multiple growing terminals and catalysts because of the halogen exchange between them, which is sometimes caused by worse

control due to the irregularity. Additionally, in this system, the phosphazene salt also possesses a halogen, which might make the halogen exchange further complicated. Thus, we examined effects of the halogen combination in the three components—initiator, iron halide, and phosphazene—on polymerization behaviors to clarify contribution of the phosphazene.

Table 2 shows polymerization results obtained with various combinations. The polymerization rate was not so sensitive for the combination, while the M_w/M_n of the prepared polymer got broader as the halogen of phosphazene was changed from Br to Cl and I for H-(MMA)₂-Br/FeBr₂ system (entries 1–3). Although each solution of the three phosphazene–halogen show colorless, the color of polymerization solution, presumably based on the in situ formed catalyst, was clearly dependent on the phosphazene–halogen: black (PZN-I), orange (PZN-Br), and yellow (PZN-Cl), which would support the formation of anionic catalyst [FeBr₂X]⁻ from the mixture of phosphazene (PZN-X). Thus, the oxidized [FeBr₃X]⁻, generated after activation of C–Br in the initiator, might sometimes return the X to growing radical, consequently giving different dormant species carrying halogen derived from the phosphazene.²¹ The worse control would be caused by such irregularity. Additionally, Cl-based species seems to be less suitable for the iron catalyst (entries 4–6), which is similar to our FeX₂(PR₃)₂-catalyzed systems.¹⁸

Comparison with Conventional Iron Catalyst: FeBr₂-(PPh₃)₂. We compared the catalytic performance of FeBr₂/PZN-Br with the conventional iron catalyst [FeBr₂(PPh₃)₂] under the same conditions. Although there was little difference in the polymerization rate, the controllability for molecular weight and its distribution was quite different (Figure 3). With the FeBr₂(PPh₃)₂, the molecular weight distributions (MWDs) were rather broad ($M_w/M_n \sim 1.70$) especially at the initial stage, and the number-average molecular weights (M_n) were larger

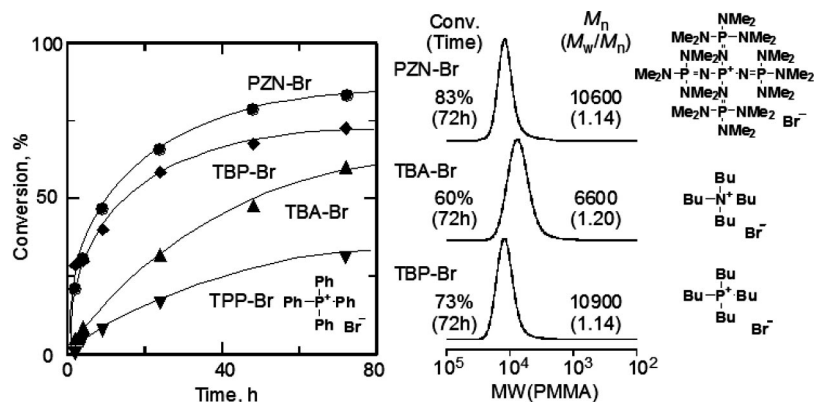


Figure 4. Comparison of onium salts for ligands of FeBr_2 on living radical polymerization of MMA in THF at 60 °C: $[\text{MMA}]_0 = 2000 \text{ mM}$; $[\text{H}-(\text{MMA})_2-\text{Br}]_0 = 20 \text{ mM}$; $[\text{FeBr}_2]_0 = 10 \text{ mM}$; $[\text{onium salt}]_0 = 10 \text{ mM}$. Onium salt: PZN-Br (●), TBA-Br (▲), TBP-Br (◆), TPP-Br (▼).

than the theoretical values, assuming that one initiator molecule generates one polymer chain. In contrast, the $\text{FeBr}_2/\text{PZN-Br}$ system gave well-controlled polymers where the M_n almost follows the theoretical line and the MWDs were narrow ($M_w/M_n < 1.20$) regardless of the monomer conversion or polymerization degree. These results show the better controllability of the $\text{FeBr}_2/\text{PZN-Br}$.

Comparison with FeBr_2 /Conventional Onium Salts. The phosphazene derivatives are categorized in onium salts. Therefore, we employed conventional onium salts such as ammonium and phosphonium derivatives in conjunction with FeBr_2 to examine the difference with phosphazene salt. Figure 4 shows the time–conversion curves of the polymerization and the SEC curves of the obtained PMMAs for a series of onium salts under the same conditions; tetrabutylammonium bromide (TBA-Br), tetrabutylphosphonium bromide (TBP-Br), and tetraphenylphosphonium bromide (TPP-Br), in addition to PZN-Br. As reported in a previous article,²¹ the combination of iron halide with onium salt is likely effective as a catalyst for living radical polymerization to give controlled polymers. However, the activity with PZN-Br was apparently higher than with the others as seen in time–conversion curve.

Cyclic Voltammetry of $\text{FeBr}_2/\text{PZN-Br}$. Observation of the redox behavior of catalysts has often supported the catalytic ability in living radical polymerization because it undergoes one-electron redox by reversibly activating carbon–halogen bond. Thus, we measured cyclic voltammetry (CV) for the $\text{FeBr}_2/\text{PZN-Br}$ complex and compared the behavior with the comparable catalysts.

For the $\text{FeBr}_2/\text{PZN-Br}$ complex, clear oxidation/reduction waves, which was likely to be assigned to one electron redox between Fe^{II} and Fe^{III} , were seen at $E_{\text{pa}} = 0.30 \text{ V}$ and $E_{\text{pc}} = 0.16 \text{ V}$, respectively (solid line, Figure 5). In addition to these, there were ambiguous peaks at from 1.0 to 1.4 V, which would be due to PZN-Br itself because they were quite similar to those observed with only PZN-Br. Importantly, the redox cycles were recurrent after several scans in the range of 0–1.4 V, indicating the trivalent species was not decomposed and can be reversibly converted into divalent one without assistance of an additive, in contrast to half-metallocene-type carbonyl iron complex $[\text{FeCpI}(\text{CO})_2]$ and ruthenium dichloride phosphine complex $[\text{RuCl}_2(\text{PPh}_3)_3]$, requiring $\text{Ti}(\text{O}i\text{-Pr})_4$ and $\text{Al}(\text{O}i\text{-Pr})_3$ for such recurrent redox cycle as well as polymerization control.^{10,26} Interestingly, the redox potential of the $\text{FeBr}_2/\text{PZN-Br}$ complex [$E_{1/2} = (E_{\text{pa}} + E_{\text{pc}})/2 = 0.23 \text{ V}$] was lower than those of conventional active catalysts such as $\text{Cp}^*(\eta\text{-C}_5\text{Me}_5)\text{-based}$ half-metallocene iron¹⁰ or ruthenium²⁷ catalysts. The dibromide phosphine catalyst $[\text{FeBr}_2(\text{PPh}_3)_2]$ showed an unclear cycle

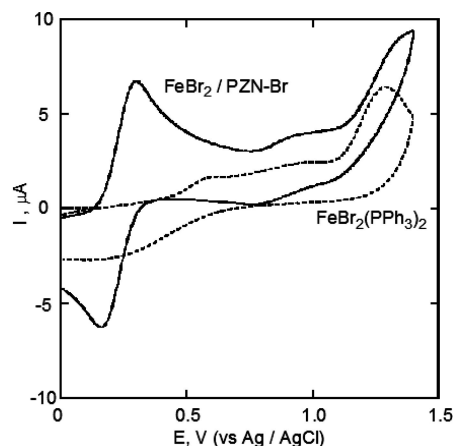


Figure 5. Cyclic voltammograms of iron catalysts in $\text{ClCH}_2\text{CH}_2\text{Cl}$ at 25 °C: $[\text{iron complex}]_0 = 5.0 \text{ mM}$, $[\text{n-Bu}_4\text{NPF}_6]_0 = 100 \text{ mM}$. Iron complex: $\text{FeBr}_2/\text{PZN-Br}$ (solid line); $\text{FeBr}_2(\text{PPh}_3)_2$ (dashed line).

(dashed line, Figure 5), and the behavior gradually changed as the measure was repeated, indicating the less stability under the redox process.

Our previous researches have indicated the trend that an enhancement of the electron density of a central metal contributes to a decrease in a redox potential and an increase in the catalytic activity.^{28,29} The mixture of FeBr_2 with PZN-Br would form an ionic catalyst $[\text{FeBr}_3]^+[\text{PZN}]^-$, and therefore the electron density of a central iron might be richer than the neutral iron catalyst $\text{FeBr}_2(\text{PPh}_3)_2$. Thus, the $\text{FeBr}_2/\text{PZN-Br}$ complex would show better catalytic performances than the neutral form for the living radical polymerization. However, we could not see the superiority of the phosphazene salt to the conventional onium salts: there was little difference of the redox behavior between them, coupled with FeBr_2 . Such ionization by an onium salt certainly seems to be effective to promote the efficiency of the redox cycle.

High Controllability of $\text{FeBr}_2/\text{PZN-Br}$ System: Monomer Addition and Synthesis of High Molecular Weight Polymer.

To investigate the living nature for the $\text{FeBr}_2/\text{PZN-Br}$ catalyzed system, we added a fresh MMA to the polymerization solution when the MMA conversion reached over 80%. In the second phase, MMA was smoothly consumed to give additional 84% conversion (totally 167%) (Figure 6). The SEC analysis of the obtained polymers showed the high controllability even after the addition, where the M_n increased in direct proportion with the conversion and the peak top was shifted to higher molecular weight keeping narrow MWD, although just a slight tailing was detected.

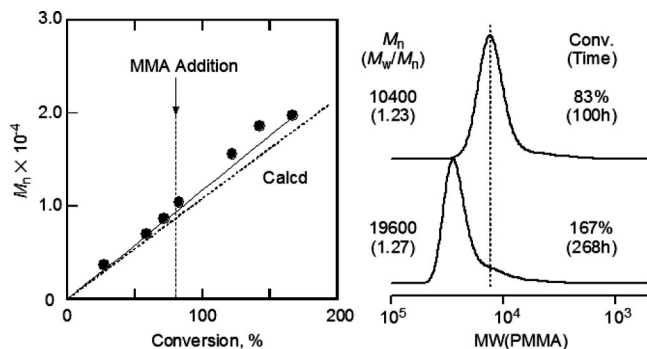


Figure 6. Monomer-addition experiments in the polymerization of MMA with $\text{H}-(\text{MMA})_2-\text{Br}/\text{FeBr}_2/\text{PZN}-\text{Br}$ in THF at 60°C : $[\text{MMA}]_0 = [\text{MMA}]_{\text{add}} = 2000 \text{ mM}$; $[\text{H}-(\text{MMA})_2-\text{Br}]_0 = 20 \text{ mM}$; $[\text{FeBr}_2]_0 = 10 \text{ mM}$; $[\text{PZN}-\text{Br}]_0 = 10 \text{ mM}$.

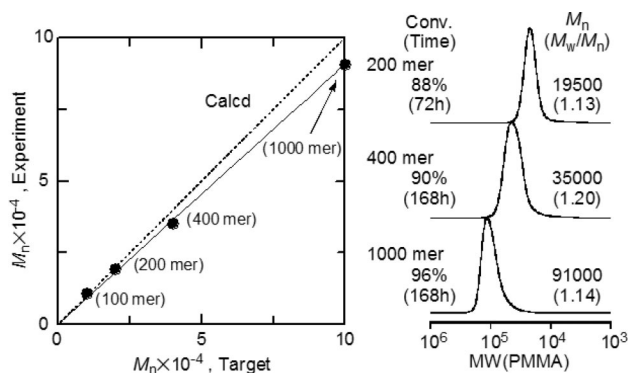


Figure 7. Synthesis of high molecular weight PMMA targeted 100-mer (A), 200-mer (B), 400-mer (C), and 1000-mer (D) with $\text{H}-(\text{MMA})_2-\text{Br}/\text{FeBr}_2/\text{PZN}-\text{Br}$ in THF at 60°C : (A) $[\text{MMA}]_0 = 2000 \text{ mM}$; $[\text{H}-(\text{MMA})_2-\text{Br}]_0 = 20 \text{ mM}$; $[\text{FeBr}_2]_0 = 10 \text{ mM}$; $[\text{PZN}-\text{Br}]_0 = 10 \text{ mM}$, (B) $[\text{MMA}]_0 = 4000 \text{ mM}$; $[\text{H}-(\text{MMA})_2-\text{Br}]_0 = 20 \text{ mM}$; $[\text{FeBr}_2]_0 = 10 \text{ mM}$; $[\text{PZN}-\text{Br}]_0 = 10 \text{ mM}$, (C) $[\text{MMA}]_0 = 4000 \text{ mM}$; $[\text{H}-(\text{MMA})_2-\text{Br}]_0 = 10 \text{ mM}$; $[\text{FeBr}_2]_0 = 5.0 \text{ mM}$; $[\text{PZN}-\text{Br}]_0 = 5.0 \text{ mM}$, (D) $[\text{MMA}]_0 = 5000 \text{ mM}$; $[\text{H}-(\text{MMA})_2-\text{Br}]_0 = 5.0 \text{ mM}$; $[\text{FeBr}_2]_0 = 5.0 \text{ mM}$; $[\text{PZN}-\text{Br}]_0 = 5.0 \text{ mM}$.

The high controllability of the $\text{FeBr}_2/\text{PZN}-\text{Br}$ system encouraged us to synthesize higher molecular weight polymers with narrow MWDs. We varied the monomer/initiator ratio from 100 to 200, 400, 1000 targeting 20 000, 40 000, 100 000 (for 100% conversion) of M_n (Figure 7). Under every condition, the MWDs of the obtained PMMAs were kept narrow ($M_w/M_n < 1.20$), and the molecular weights agreed well with the theoretical values, calculated from the feed ratio and the conversion, even for nearly 100 000 of M_n . These results indicate that the $\text{FeBr}_2/\text{PZN}-\text{Br}$ was highly active for living radical polymerization of MMA and effective for wide range of molecular weight control.

Polymerization of Functional Monomer. Most conventional iron catalysts interact with functional groups (e.g., ethylene glycol, hydroxyl, amino, and carboxyl groups, etc.), and thus they unfavorably turn into “deactivation” to lose the catalysis for monomers bearing such functional groups, although such functional monomers are essential for preparation of advanced polymeric materials. Here, we applied the ionic catalyst, generated from FeBr_2 and $\text{PZN}-\text{Br}$, to polymerization of one of functional methacrylates, PEGMA, carrying a poly(ethylene glycol) pendant group, coupled with $\text{H}-(\text{MMA})_2-\text{Br}$ as an initiator in toluene at 60°C .

In sharp contrast to little activity of the conventional iron catalyst $[\text{FeBr}_2(\text{PPh}_3)_2]$, as seen in the time–conversion curve in Figure 8, the $\text{FeBr}_2/\text{PZN}-\text{Br}$ catalyst showed higher activity even for such functional monomer, where PEGMA was

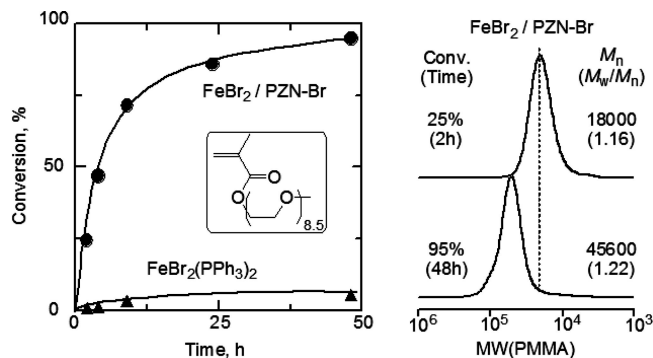


Figure 8. Comparison of $\text{FeBr}_2/\text{PZN}-\text{Br}$ with $\text{FeBr}_2(\text{PPh}_3)_2$ on living radical polymerization of PEGMA in toluene at 60°C : $[\text{PEGMA}]_0 = 500 \text{ mM}$; $[\text{H}-(\text{MMA})_2-\text{Br}]_0 = 5 \text{ mM}$; $[\text{iron catalyst}]_0 = 5 \text{ mM}$. Iron catalyst: $\text{FeBr}_2/\text{PZN}-\text{Br}$ (●); $\text{FeBr}_2(\text{PPh}_3)_2$ (▲).

smoothly polymerized in high conversion ($>90\%$) for 40 h without retardation. The SEC curves of the obtained poly(PEGMA) was shifted to higher molecular weight with the monomer conversion, and the molecular weight distributions were relatively narrow regardless of the conversion ($M_w/M_n < 1.25$). The bulky and conjugated structure of phosphazene ligand would contribute to the protection of the iron center against polar functional groups, which is now under investigation in detail.

Removal of Catalyst. Finally, we examined the removability of the $\text{FeBr}_2/\text{PZN}-\text{Br}$ catalyst from the products after the polymerization of MMA. The polymerization solution expressed rust color derived from the catalyst, but only water washing, followed by dilution with toluene, made the solution colorless. The ICP-AES (inductively coupled plasma–atomic emission spectrometry) analysis of the obtained polymer after three-times washing showed that it contained less than 5 ppm iron, namely nearly perfect removability of the catalyst.

Conclusions

We have showed phosphazanium bromide ($\text{PZN}-\text{Br}$) with FeBr_2 was effective as a catalyst for living radical polymerization of MMA. The catalytic performance was maximized with an equimolar mixture of the both, indicating they would form an equimolar anionic complex. The $\text{FeBr}_2/\text{PZN}-\text{Br}$ catalyst possessed higher activity/controllability than a conventional iron catalyst $[\text{FeBr}_2(\text{PPh}_3)_2]$ or the combinations with other conventional onium–halogen salts, demonstrated by the successful chain extension by monomer addition and fine control even for high molecular weight polymer ($M_n \sim 90\,000$; $M_w/M_n < 1.20$). More importantly, the catalyst showed high activity even for living polymerization of PEGMA, one of the functional methacrylates, which is quite distinguished from previous iron catalysts. Despite such tolerance to functional groups, the catalyst was almost quantitatively removed by just water-washing. Therefore, the catalyst would open the door to new development for actual application of iron-catalyzed living radical polymerization.

Acknowledgment. We thank Takeshi Niitani and his colleagues of Nippon Soda Co. Ltd. for ICP-AES analysis. This research was partially supported by the Ministry of Education, Science, Sports and Culture, Grant-in-Aid for Creative Scientific Research (18GS0209).

References and Notes

- (1) This work was presented in part at the following meetings: The 55th Symposium on Macromolecules, the Society of Polymer Science, Toyama, Japan, Sept 2006; paper 2B10: Ishio, M.; Katsube, M.; Ouchi, M.; Sawamoto, M.; Inoue, Y. *Polym. Prepr. Jpn.* **2006**, 55 (2), 2443.

- (2) Bolm, C.; Legros, J.; Paih, J. L.; Zani, L. *Chem. Rev.* **2004**, *104*, 6217–6254.
- (3) (a) Kato, M.; Kamigaito, M.; Sawamoto, M.; Higashimura, T. *Macromolecules* **1995**, *28*, 1721–1723. (b) Ando, T.; Kato, M.; Kamigaito, M.; Sawamoto, M. *Macromolecules* **1996**, *29*, 1070–1072.
- (4) For recent reviews on transition-metal-catalyzed living radical polymerization, see: (a) Kamigaito, M.; Ando, T.; Sawamoto, M. *Chem. Rev.* **2001**, *101*, 3689–3745. (b) Kamigaito, M.; Ando, T.; Sawamoto, M. *Chem. Rev.* **2004**, *4*, 159–175. (c) Matyjaszewski, K.; Xia, J. *Chem. Rev.* **2001**, *101*, 2921–2990. (d) *Controlled/Living Radical Polymerization From Synthesis to Materials*; Matyjaszewski, K., Ed.; ACS Symposium Series 944; American Chemical Society: Washington, DC, 2006.
- (5) Wang, J. S.; Matyjaszewski, K. *J. Am. Chem. Soc.* **1995**, *117*, 5614–5615.
- (6) Granel, C.; Dubois, P.; Jerome, R.; Teyssie, P. *Macromolecules* **1996**, *29*, 8576–8582.
- (7) Ando, T.; Kamigaito, M.; Sawamoto, M. *Macromolecules* **1997**, *30*, 4507–4510.
- (8) Matyjaszewski, K.; Wei, M.; Xia, J.; McDermott, N. E. *Macromolecules* **1997**, *30*, 8161–8164.
- (9) Kotani, Y.; Kamigaito, M.; Sawamoto, M. *Macromolecules* **1999**, *32*, 6877–6880.
- (10) Kotani, Y.; Kamigaito, M.; Sawamoto, M. *Macromolecules* **2000**, *33*, 3543–3549.
- (11) Zhu, S.; Yan, D. *Macromolecules* **2000**, *33*, 8233–8238.
- (12) Louie, Y.; Grubbs, R. H. *Chem. Commun.* **2000**, 1479–1480.
- (13) Gibson, V. C.; O'Reilly, R. K.; Reed, W.; Wass, D. F.; White, A. J. P.; Williams, D. J. *Chem. Commun.* **2002**, 1850–1851.
- (14) Göbelt, B.; Matyjaszewski, K. *Macromol. Chem. Phys.* **2000**, *201*, 1619–1624.
- (15) O'Reilly, R. K.; Gibson, V. C.; White, A. J. P.; Williams, D. J. *J. Am. Chem. Soc.* **2003**, *125*, 8450–8451.
- (16) Xue, Z.; Lee, B. W.; Noh, S. K.; Lyoo, W. S. *Polymer* **2007**, *48*, 4704–4714.
- (17) Niibayashi, S.; Hayakawa, H.; Jin, R.-H.; Nagashima, H. *Chem. Commun.* **2007**, 1855–1857.
- (18) Uchiike, C.; Terashima, T.; Ouchi, M.; Ando, T.; Kamigaito, M.; Sawamoto, M. *Macromolecules* **2007**, *40*, 8658–8662.
- (19) Ferro, R.; Milione, S.; Bertolasi, V.; Capacchione, C.; Grassi, A. *Macromolecules* **2007**, *40*, 8544–8546.
- (20) Furuyama, R.; Fujita, T.; Funaki, S. F.; Nobori, T.; Nagata, T.; Fujiwara, K. *Catal. Surveys Asia* **2004**, *8*, 61–71.
- (21) Teodorescu, M.; Gaynor, S. G.; Matyjaszewski, K. *Macromolecules* **2000**, *33*, 2335–2339.
- (22) Ando, T.; Kamigaito, M.; Sawamoto, M. *Macromolecules* **2000**, *33*, 2819–2824.
- (23) Ando, T.; Kamigaito, M.; Sawamoto, M. *Tetrahedron* **1997**, *53*, 15445–15457.
- (24) Nobori, T.; Kouno, M.; Suzuki, T.; Mizutani, K.; Kiyono, S.; Sonobe, Y.; Takaki, U. Phosphazanium salt and preparation process thereof, and process for producing poly(alkylene oxide). U.S. 5,990,352, **1999**.
- (25) Iron dichloride (FeCl_2) is known to form a dinuclear anionic compound (Fe_2Cl_6)²⁻ with 1 equiv of onium chloride salt: Sun, J. S.; Zhao, H.; Ouyang, X.; Clérac, R.; Smith, J. A.; Clemente-Juan, J. M.; Gómez-García, C.; Coronado, E.; Dunbar, K. R. *Inorg. Chem.* **1999**, *38*, 5841–5855. On the basis of this paper, we suppose that the equimolar mixture of FeBr_2 and phosphazanium salt (PZN-X) also generates similar anionic complex. However, we have never examined the detailed structure or whether it exists with monomeric or dimeric form. Thus, we just describe the forming complex as $[\text{FeBr}_2\text{X}]^-$ in this paper.
- (26) Ando, T.; Kamigaito, M.; Sawamoto, M. *Macromolecules* **2000**, *33*, 6732–6737.
- (27) Ando, T.; Kamigaito, M.; Sawamoto, M. *Macromolecules* **2000**, *33*, 5825–5829.
- (28) Takahashi, H.; Ando, T.; Kamigaito, M.; Sawamoto, M. *Macromolecules* **1999**, *32*, 3820–3823.
- (29) Kamigaito, M.; Watanabe, Y.; Ando, T.; Sawamoto, M. *J. Am. Chem. Soc.* **2002**, *124*, 9994–9995.

MA801762K